arXiv:1401.3777v2 [cond-mat.quant-gas] 26 Sep 2014

Dark Solitons with Majorana Fermions in Spin-Orbit-Coupled Fermi Gases

Yong Xu[1],* Li Mao[2,1],* Biao Wu[3,4], and Chuanwei Zhang[1]†
[1]*Department of Physics, The University of Texas at Dallas, Richardson, Texas 75080, USA*
[2]*School of Physics and Technology, Wuhan University, Wuhan 430072, China*
[3]*International Center for Quantum Materials, School of Physics, Peking University, Beijing 100871, China and*
[4]*Collaborative Innovation Center of Quantum Matter, Beijing 100871, China*

We show that a single dark soliton can exist in a spin-orbit-coupled Fermi gas with a high spin imbalance, where spin-orbit coupling favors uniform superfluids over non-uniform Fulde-Ferrell-Larkin-Ovchinnikov states, leading to dark soliton excitations in highly imbalanced gases. Above a critical spin imbalance, two topological Majorana fermions (MFs) without interactions can coexist inside a dark soliton, paving a way for manipulating MFs through controlling solitons. At the topological transition point, the atom density contrast across the soliton suddenly vanishes, suggesting a signature for identifying topological solitons.

PACS numbers: 03.75.Ss, 03.75.Lm

Solitons, topological defects arising from the interplay between dispersion and nonlinearity of underlying systems, are significant for many different physical branches [1–4]. The realization of cold atomic superfluids provides a clean and controllable platform for exploring soliton physics. In cold atomic gases, dark solitons represent quantum excitations of a superfluid with the superfluid order parameter vanishing at the soliton center in conjunction with a phase jump across the soliton. Dark solitons have been extensively investigated in cold atoms [5–13]. In particular, dark solitons have recently been experimentally observed in strongly interacting spin balanced Fermi gases [14], where the Cooper pairing wave-function has a phase jump across the soliton [15–21]. However, dark solitons in the presence of a large spin imbalance have not been well explored.

With a large spin imbalance, the ground state of the superfluid is theoretically predicted to be the spatially non-uniform Fulde-Ferrell-Larkin-Ovchinnikov (FFLO) phase [22] with finite momentum pairing in 1D and quasi-1D [23–28], which is partially verified by the experiment [29]. This spatially non-uniform phase does not support dark soliton excitations that usually occur in BCS-type uniform superfluids. On the other hand, uniform superfluids can exist in large spin imbalanced Fermi gases [30] in the presence of spin-orbit (SO) coupling. Since SO coupling for cold atoms has been experimentally generated recently for both bosons and fermions [31–36], a natural question is whether such SO coupled superfluids with large spin imbalances can also support dark solitons.

More interestingly, it is well known that defects (vortices, edges, etc.) in SO coupled fermionic superfluids with large spin imbalances can accommodate Majorana fermions (MFs) [37–42], topological excitations that satisfy exotic non-Abelian exchange statistics [43]. Recently MFs have attracted tremendous attention in various physical systems [44] because of their fundamental importance as well as potential applications in fault-tolerant quantum computation [45]. In this context, SO coupled fermionic superfluids have their intrinsic advantages for MFs because of their disorder free [46] and highly controllable characteristics. Therefore another important question is whether topological Majorana excitations can exist inside dark solitons if such topological defects do exist.

In this Letter, we address these two important questions by studying dark solitons in degenerate Fermi gases (DFGs) trapped in 1D harmonic potentials with the experimentally already realized SO coupling and spin imbalances. Here the spin imbalance is equivalent to a Zeeman field. In the absence of SO coupling, the FFLO state [22] with an oscillating order parameter amplitude is the ground state [24] with a large Zeeman field, which cannot support dark solitons. With SO coupling, we find

(i) SO coupling suppresses the FFLO state, leading to uniform BCS superfluids that support dark solitons. The parameter region for dark solitons and their spatial properties are obtained.

(ii) For substantially large spin imbalances, we find remarkably that two MFs can coexist inside a dark soliton without any interaction, beyond the general expectation that two MFs with overlapping wave-functions interact, leading to energy splitting that destroys MFs. Such solitons are topological solitons to be distinguished from solitons without MFs.

(iii) The experimental signature of MFs inside the dark soliton in the local density of states (LDOS) is characterized, which show an isolated zero energy peak at the center of the soliton. Moreover, the density contrast across the soliton suddenly decreases to zero at the topological transition point, which may be used to experimentally detect topological solitons.

System and Hamiltonian: Consider a SO coupled DFG confined in a 1D harmonic trap with the transversal confinement provided by a tightly focused optical dipole trap. The many-body Hamiltonian of the system can

be written as

$$H = \int dx \hat{\Psi}^\dagger(x) H_s \hat{\Psi}(x) \quad (1)$$
$$-g \int dx \hat{\Psi}^\dagger_\uparrow(x) \hat{\Psi}^\dagger_\downarrow(x) \hat{\Psi}_\downarrow(x) \hat{\Psi}_\uparrow(x),$$

where the single particle grand-canonical Hamiltonian $H_s = -\hbar^2\partial_x^2/2m - \mu + V(x) + H_{\rm SOC} + H_z$, the harmonic trapping potential $V(x) = m\omega^2 x^2/2$, μ is the chemical potential, g is the attractive s-wave scattering interaction strength between atoms that can be tuned through Feshbach resonances, m is the atom mass, and ω is the trapping frequency. $\hat{\Psi}(x) = [\hat{\Psi}_\uparrow(x), \hat{\Psi}_\downarrow(x)]^T$ with the atom creation (annihilation) operator $\hat{\Psi}^\dagger_\nu(x)$ ($\hat{\Psi}_\nu(x)$) at spin ν and position x. We consider the equal Rashba and Dresselhaus SO coupling $H_{SOC} = -i\hbar\alpha\partial_x\sigma_y$, where σ_i are Pauli matrices. The Zeeman field $H_z = V_z\sigma_z$ generates the spin imbalance. This type of SO coupling and Zeeman field have been realized experimentally [31–36] for cold atom Fermi gases using two counter-propagating Raman lasers that couple two atomic hyperfine ground states (i.e., the spin).

Within the standard mean-field approximation, the fermionic superfluids can be described by the Bogoliubov-de Gennes (BdG) equation

$$\begin{pmatrix} H_s & \Delta(x) \\ \Delta(x)^* & -\sigma_y H_s^* \sigma_y \end{pmatrix} \begin{pmatrix} u_n \\ v_n \end{pmatrix} = E_n \begin{pmatrix} u_n \\ v_n \end{pmatrix}, \quad (2)$$

where $u_n = [u_{n\uparrow}(x), u_{n\downarrow}(x)]^T$, $v_n = [v_{n\downarrow}(x), -v_{n\uparrow}(x)]$ are the Nambu spinor wave-functions for the quasi-particle excitation energy E_n, the order parameter $\Delta(x) = -g\langle\hat{\Psi}_\downarrow(x)\hat{\Psi}_\uparrow(x)\rangle = -(g/2)\sum_{|E_n|<E_c}\left[u_{n\uparrow}v^*_{n\downarrow}f(E_n) + u_{n\downarrow}v^*_{n\uparrow}f(-E_n)\right]$, and the atom density $\rho_\sigma(x) = (1/2)\sum_{|E_n|<E_c}\left[|u_{n\sigma}|^2 f(E_n) + |v_{n\sigma}|^2 f(-E_n)\right]$ with the energy cut-off E_c. $f(E) = 1/(1+e^{E/k_BT})$ is the quasi-particle Fermi-Dirac distribution at the temperature T. With the constraints of a fixed total number of atoms $N = \int dx\,[\rho_\uparrow(x) + \rho_\downarrow(x)]$ and the definition of the order parameter, Eq. (2) can be solved self-consistently. To obtain a stationary soliton excitation in the superfluid, we choose $\Delta\tanh(x/\xi)$ with coherent length $\xi = \hbar v_F/\Delta$ and Fermi velocity $v_F = \hbar K_F/m$ as the initial order parameter, and then solve the BdG equations self-consistently until the order parameter and density converge.

To solve the BdG equation, we expand u_n and v_n on the basis states of the harmonic oscillator to convert the equation to a diagonalization problem of a secular matrix. We consider $N = 100$ atoms with 300 harmonic oscillator states for the wave-function expansion. The energy cut-off $E_c = 240\hbar\omega$, which is large enough to ensure the accuracy of the calculation [24]. We choose the single particle Fermi energy $E_F = N\hbar\omega/2$ (neglecting zero point energy) in the absence of the SO coupling and Zeeman field and the harmonic oscillator length $x_s = \sqrt{\hbar/m\omega}$ as the units of energy and length. For 1D Fermi gases, the interaction parameter $g = -2\hbar^2/ma_{1D}$ with an effective 1D scattering length a_{1D} [29]. A dimensionless parameter $\Gamma = -mg/n(0)\hbar^2 = \pi x_s/\sqrt{N}a_{1D}$, which is proportional to the ratio between the interaction and kinetic energy at the center, can be used to characterize the interaction strength [24]. Here $n(0)$ is the density at the trap center in Thomas-Fermi approximation. In experiments [29], this value can be as large as 5.2. We choose $\Gamma = \pi$ in most of our calculations.

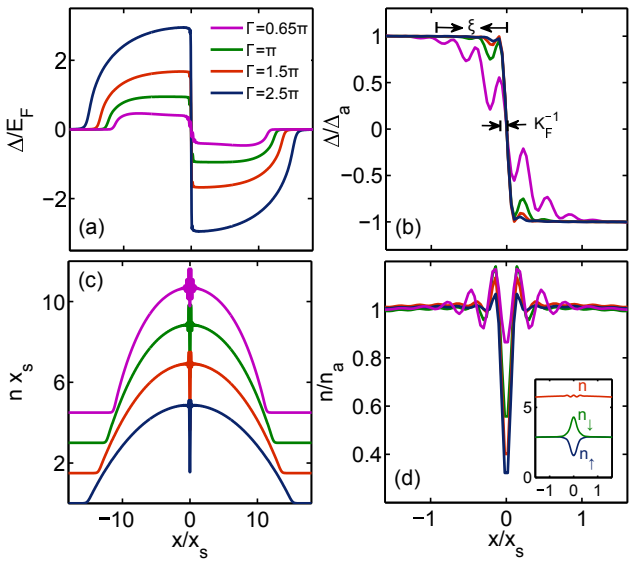

FIG. 1: (Color online) Profiles of the order parameter Δ ((a) and (b)) and the total density n ((c) and (d)) with increasing atom interactions. In (b) and (d), the details of dark solitons in a small region are plotted, where Δ and n are respectively scaled by Δ_a and n_a, which are the asymptotic value to the origin point without the soliton. In (c), lines corresponding to $\Gamma = 1.5\pi, \pi, 0.65\pi$ are moved up $1.5x_s, 3.0x_s, 4.5x_s$ with respect to the line for $\Gamma = 2.5\pi$. In the inset of (d), the density profiles (n_σ for spin σ and $n = n_\uparrow + n_\downarrow$) for a gas with $\Gamma = \pi$ without SO coupling are plotted. Here $\alpha k_F = E_F$ and $V_z = 0.16E_F$.

Dark solitons in spin imbalanced DFGs: In Fig. 1, we plot the order parameter and density profiles for an imbalanced SO coupled Fermi gas with different interaction strengths. With increasing interactions, both Δ and the depth of the soliton increase while μ (not shown here) decreases, signalling the crossover from BCS superfluids to BEC molecule bound states. Without SO coupling, the existence of a dark soliton leads to the depletion (enhancement) of spin $\uparrow$ ($\downarrow$) component even with small Zeeman fields, thus the total atom density only has a small depletion at the soliton center as shown in the inset of Fig. 1(d). This is in sharp contrast to Fig. 1(c,d) with SO coupling, where a strong deple-

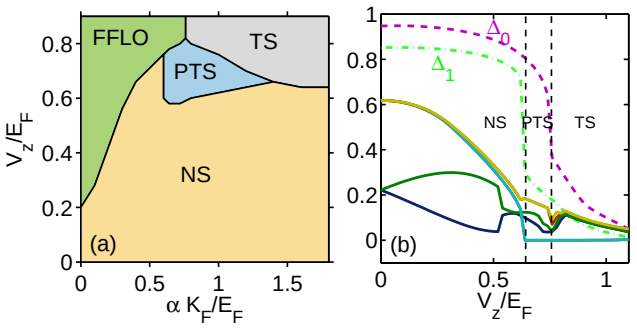

FIG. 2: (Color online) (a) Phase diagram in the (α, V_z) plane. PTS: partial topological superfluid; TS: topological superfluid; NS: normal superfluid. (b) Quasi-particle excitation energies (all other lines except light green dashed-dotted and magenta dashed lines) and Δ_0 (maximum of the order parameter in whole region), Δ_1 (minimum of the order parameter in region $(2x_s < x < 9x_s)$, where the topological superfluids exist). $\alpha K_F = E_F$ and $\Gamma = \pi$.

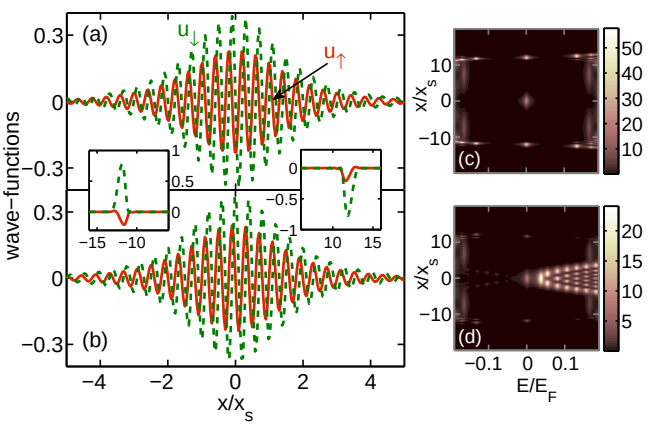

FIG. 3: (Color online) The left panel shows the wavefunctions (solid red line for $u_\uparrow$ and dashed green one for $u_\downarrow$) of four MFs: two inside the dark soliton plotted in (a) and (b) and two at the edges in the insets. (c) and (d) show the local density of states for spin $\downarrow$ and spin $\uparrow$ respectively. Here $V_z = 0.768E_F$, $\alpha K_F = E_F$, and $\Gamma = \pi$.

tion of the total density (also for each spin component) in the dark soliton is observed. In Fig. 1(b), we observe two length scales for the dark soliton. One is K_F^{-1} defined using the local density approximation, corresponding to the steep slope and the oscillation wavelength. The other is the coherence length, corresponding to the smoother oscillation slope [16, 47], which is about $5K_F^{-1}, 2.2K_F^{-1}, 1.2K_F^{-1}, K_F^{-1}$ for $\Gamma = 0.65\pi, \pi, 1.5\pi, 2.5\pi$, respectively. These two scales are equivalent in the BEC limit, where the oscillation structure of the soliton vanishes.

The physical mechanism for the dark soliton in an imbalanced Fermi gas roots in the SO coupling. Without SO coupling, the ground state of a 1D imbalanced Fermi gase in a harmonic trap is predicted to possess the two-shell structure: partially polarized core (i.e. FFLO state) surrounded by either a paired or a fully polarized phase [24, 28]. This two-shell structure has been partially verified in the experiment [29]. With SO coupling, the FFLO state is dramatically suppressed as shown in Fig. 2(a) because the BCS type of zero total momentum Cooper pairing can be formed in the same helicity band, which is energetically preferred than the FFLO state that is formed through the pairing between atoms in two different helicity bands [48, 49] with non-zero total momentum. A dark soliton can be created in the BCS type of phases, but not in the FFLO phase, where the stable state generated by phase imprinting is also an oscillating FFLO state with a sinusoidal-like form and has lower energy than a soliton state. In this sense, SO coupling makes it possible to generate a single dark soliton excitation with a high spin imbalance.

Two MFs inside a dark soliton: There are two topological superfluid (TS) phases in Fig. 2(a): partial TS (PTS) phase, where the superfluid has a phase separation structure with a normal superfluid core surrounded by a TS, and TS phase, where the whole region is topological. The phase separation in the PTS phase originates from the harmonic trapping geometry, where the chemical potential is replaced by a local one $\bar{\mu}(x) = \mu - V(x)$ using the local density approximation. For a homogeneous gas, superfluids become topological when $V_z > \sqrt{\mu^2 + \Delta^2}$ [38, 39] with Majarona zero modes located at the edges. For a harmonically trapped gas, as the chemical potential decreases from the trap center to edge, the condition $V_z > \sqrt{\bar{\mu}^2(x) + \Delta^2}$ [41] (See supplementary materials) is first satisfied at the wings of the superfluids ($V_z < \sqrt{\mu^2 + \Delta^2}$ at the trap center) for the PTS phase. This transition is characterized by the appearance of two zero energy modes (cyan line and red one hidden behind the cyan in Fig. 2(b)) located around the place with $V_z = \sqrt{\bar{\mu}^2 + \Delta^2}$, and the sharp decrease of the order parameter in the topological region (Δ_1 in Fig. 2(b)). As V_z is furthur increased with $V_z > \sqrt{\mu^2 + \Delta^2}$, the whole superfluids become topological (TS phase) as the maximum of the order parameter (Δ_0) drops suddenly. Without a soliton, there is only one zero energy mode in TS phase. However, a soliton induces another zero energy mode. This additional zero energy mode is different from conventional local gapped excitations (blue and green lines in Fig. 2(b)) that are similar to Andreev bound states in a vortex [16, 47]. It appears only when the local superfluid, where the soliton is located, becomes topological.

To confirm that the additional zero energy state is MFs inside the soliton, we consider a linear combination of the Bogoliubov quasi-particle operators γ_{0^n} for states with $E_n \sim 0$ (here $E_2 > E_1$ correspond to cyan and red lines respectively) to obtain spatially localized states: $\gamma_L = (\gamma_{0^{+2}} + \gamma_{0^{+1}} + \gamma_{0^{-2}} + \gamma_{0^{-1}})/2$, $\gamma_R = (\gamma_{0^{+2}} - \gamma_{0^{+1}} + \gamma_{0^{-2}} - \gamma_{0^{-1}})/2$, $\gamma_{S1} = (\gamma_{0^{+2}} - \gamma_{0^{-2}})/2i$,

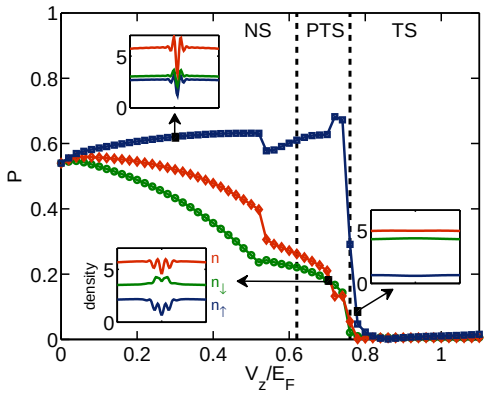

FIG. 4: (Color online) Density contrast P_σ as a function of V_z for the spin $\downarrow$ (circle green line), spin $\uparrow$ (square blue line), and total (diamond red line) densities in the soliton region $-1.5x_s < x < 1.5x_s$. The insets show the density profiles (n_σ for spin σ and $n = n_\uparrow + n_\downarrow$) of the soliton in each region with the unit $1/x_s$, corresponding to $V_z = 0.3E_F, 0.7E_F, 0.768E_F$ respectively. Here $\alpha K_F = E_F$ and $\Gamma = \pi$.

$\gamma_{S2} = (\gamma_{0^{+1}} - \gamma_{0^{-1}})/2i$. Due to the particle-hole symmetry $\gamma_{0^n} = \gamma^\dagger_{0^{-n}}$, we obtain $\gamma^\dagger_L = \gamma_L$, $\gamma^\dagger_R = \gamma_R$, and $\gamma^\dagger_{S\sigma} = \gamma_{S\sigma}$ with $\sigma = 1, 2$, indicating that γ_L, γ_R and $\gamma_{S\sigma}$ are self Hermitian Majorana operators. In Fig. 3(a,b), we plot the wave-functions of MFs, showing that two MFs at the left and right edges (two insets) and two MFs inside the soliton ((a) and (b)). The wave-functions of MFs inside the soliton behave like $\sim \cos(\pi K_F x/2)\exp(-x^2/\xi_0^2)$ and $\sim \sin(\pi K_F x/2)\exp(-x^2/\xi_0^2)$, similar to Andreev bound states [16] but with ξ_0 larger than ξ. They are very different from widely known MFs in vortices or nanowire ends that interact due to the wave-function overlap, leading to energy splitting that destroys the zero energy states. The vanishing interaction between MFs inside the dark soliton is due to the intrinsic property of a dark soliton: a sharp phase change. We can understand this through Kitaev's toy model [50], and the interaction is proportional to $-i\frac{t}{2}\cos(\delta\phi/2)\gamma_{S1}\gamma_{S2}$ if written in the Majorana fermion representation with the phase difference $\delta\phi$ between two sides of the soliton. For a dark soliton, $\delta\phi = \pi$ and there is no interaction. Such coexistence of two MFs inside a soliton makes it possible to drag MFs to a new position given that a dark soliton can be manipulated by means of optical lattices [51].

Evolution of soliton structure: The soliton structure can be characterized by the density contrast $P_\sigma = (n^\sigma_{\max} - n^\sigma_{\min})/n^\sigma_{\max}$ with the maximum $n^\sigma_{\max}$ and minimum $n^\sigma_{\min}$ of the density for spin σ (P_t for the total density) in the soliton region. In Fig. 4, we plot P_σ as a function of V_z. We see both $P_\downarrow$ and P_t decrease, while $P_\uparrow$ is almost a constant with increasing V_z before the appearance of MFs inside the soliton in the TS region. However, the soliton structure almost vanishes in the TS region with two MFs accommodating the soliton. The sudden decrease of the density contrast at the topological transition point is mainly due to the sharp decrease of the pairing order parameter, as shown by Δ_0 in Fig. 2(b), leading to the sudden decrease of the number of atoms participating in the pairing around the soliton. The sudden disappearance of the density contrast across the dark soliton might provide an experimental signature for the appearance of MFs inside the dark soliton. From the insets, we see that the soliton density $n_\downarrow$ has a convex structure for $V_z > 0.53E_F$, where the density inside the soliton is larger than its surrounding. The transition to this convex structure leads to the kinks around $V_z = 0.53E_F$ observed in Fig. 2(b) and Fig. 4. This convex structure of soliton density is caused by the local quasi-particle excitations. In fact, without taking into account of such quasi-particle contributions to the density, $P_\downarrow$ is almost zero.

Experimental signature of topological solitons and MFs: In the right panel of Fig. 3, we present the local density of states [24] of the Fermi gas, $\rho_\sigma(x, E) = \sum_{|E_n|<E_c}\left[|u_{n\sigma}|^2\delta(E - E_n) + |v_{n\sigma}|^2\delta(E + E_n)\right]/2$ with $\sigma = \uparrow, \downarrow$, which reflect the zero energy excitations at the places where MFs are locally accommodated. Clearly, in the TS region, the zero energy MF states appear at $x = 0$, where the dark soliton locates. In experiments, the LDOS could be measured using spatially resolved radio-frequency (rf) spectroscopy [52] with the space resolution about $1.4\mu m$ and spectral resolution about $0.5kHz$ that are smaller than the space resolution $5.4\mu m$ and energy resolution $3kHz$ shown in Fig. 3(c, d) [29]. The LDOS in a dark soliton in the trap center provides a stronger and stabler signal than that at the edges with small atom densities around MFs [41].

The 1D SO coupling and Zeeman fields considered here have already been achieved for ^{40}K and ^{6}Li fermionic atoms by coupling two hyperfine ground states using two Raman laser beams in experiments [32, 33, 36]. In experiment, the SO coupling and Zeeman field strength can be tuned through varying the laser intensity or the setup of the laser beams. The SO coupling can be as large as $\alpha K_F \sim E_F$ and a Zeeman field can be readily tuned to $V_z \sim E_F$. The realization of 1D Fermi gases and the dark soliton can be similar as that in recent experiments [14], where an elongated 1D Fermi gas is confined in a harmonic trap with cylindrical symmetry (radial trapping frequency much larger than axial one) using a combination of weak magnetic trap (axial) and tightly focused optical trap (radial). Dark solitons can be experimentally created via phase imprinting [11, 12, 14], where a half of the cloud is shortly interacted with a laser beam to acquire the phase difference.

Discussion: The mean-field BdG theory used here may give a qualitative description of the 1D physics. In particular, for 1D Fermi gases with weak and moderate interactions, the energy and chemical potential obtained from mean-field theory and exact Bethe ansatz were compared

[24] and only small discrepancy was found. Moreover, the fluctuations could be suppressed in an experimentally trapped Fermi gas, where the density of states is a constant, similar to homogenous 2D systems [24]. For a SO coupled Fermi gas, recent comparison between the mean-field phase diagram and the exact 1D DMRG simulation shows the qualitative correctness of the mean-field approximation [53]. Furthermore, quasi-1D Fermi gases can be engineered via an externally imposed strong optical lattice in experiments [29] and the weak tunneling [25, 27, 54] along transverse directions can be tuned to suppress the fluctuations. For solitons in highly elongated DFGs, the experimentally observed long period of the soliton oscillation was found to be in good agreement with the hydrodynamic theory [14], which is an approximation of the mean-field BdG approach. Our work provides the first step approach to understand the fundamental soliton physics in this system, and more quantitative results need further investigation.

To conclude, we showed that a single dark soliton excitation can exist in an imbalanced DFG with SO coupling, in sharp contrast to the FFLO state without SO coupling. With a substantial spin imbalance, we found that two MFs can coexist inside one single dark soliton without interactions, which provides a new avenue for experimentally observing and manipulating MFs by controlling solitons as well as creating Majorana trains by engineering soliton trains [55].

Acknowledgement: We would like to thank X. Liu, R. Chu, and M. J. H. Ku for helpful discussions. Y. Xu, L. Mao, and C. Zhang are supported by ARO(W911NF-12-1-0334), AFOSR (FA9550-13-1-0045), and NSF-PHY (1249293). L. Mao is also supported by the NSF of China (11344009). B. Wu is supported by the NBRP of China (2013CB921903,2012CB921300) and the NSF of China (11274024,11334001). We also thank Texas Advanced Computing Center, where our program is performed.

* These authors contributed equally to the work
† Corresponding Author, Email: chuanwei.zhang@utdallas.edu

[1] P. G. Drazin and R. S. Johnson, Solitons: An Introduction, Cambridge University Press, Cambridge, 2002.
[2] L. A. Dickey, soliton equations and Hamiltonian systems, World Scientific Press, New York, 2003.
[3] Y. S. Kivshar and G. P. Agrawal, Optical solitons, Academic Press, San Diego, 2003.
[4] P. G. Kevrekidis, D. J. Frantzeskakis, and R. Carretero-González, Emergent Nonlinear Phenomena in Bose-Einstein Condensates, Springer, 2007.
[5] L. D. Carr, M. A. Leung, and W.P. Reinhardt, J. Phys. B **33**, 3983 (2000).
[6] A. D.Jackson, G. M. Kavoulakis, and C.J. Pethick, Phys. Rev. A **58**, 2417 (1998).
[7] R. Dum, J. I. Cirac, M. Lewenstein, and P. Zoller, Phys. Rev. Lett. **80**, 2972 (1998).
[8] A. E. Muryshev, H. B. van Linden van den Heuvell, and G. V. Shlyapnikov, Phys. Rev. A **60**, R2665 (1999).
[9] P. O. Fedichev, A. E. Muryshev, and G. V. Shlyapnikov, Phys. Rev. A **60**, 3220 (1999).
[10] V. Achilleos, J. Stockhofe, P. G. Kevrekidis, D. J. Frantzeskakis, and P. Schmelcher, Eur. Phys. Lett. **103**, 20002 (2013).
[11] S. Burger, K. Bongs, S. Dettmer, W. Ertmer, K. Sengstock, A. Sanpera, G. V. Shlyapnikov, and M. Lewenstein, Phys. Rev. Lett. **83**, 5198 (1999).
[12] J. Denschlag, J. E. Simsarian, D. L. Feder, C. W. Clark, L. A. Collins, J. Cubizolles, L. Deng, E. W. Hagley, K. Helmerson, W. P. Reinhardt, S. L. Rolston, B. I. Schneider, and W. D. Phillips, Science **287**, 97 (2000).
[13] B. P. Anderson, P. C. Haljan, C. A. Regal, D. L. Feder, L. A. Collins, C. W. Clark, and E. A. Cornell, Phys. Rev. Lett. **86**, 2926 (2001).
[14] T. Yefsah, A. T. Sommer, M. J. H. Ku, L. W. Cheuk, W. Ji, W. S. Bakr, and M. W. Zwierlein, Nature (London) **499**, 426 (2013); M. J. H. Ku, W. Ji, B. Mukherjee, E. Guardado-Sanchez, L. W. Cheuk, T. Yefsah, and M. W. Zwierlein, Phys. Rev. Lett. **113**, 065301 (2014). The observed dark soliton was later confirmed to be a soliton vortex.
[15] J. Dziarmaga and K. Sacha, Laser Phys. **15**, 674 (2005).
[16] M. Antezza, F. Dalfovo, L. P. Pitaevskii, and S. Stringari, Phys. Rev. A **76**, 043610 (2007).
[17] R. G. Scott, F. Dalfovo, L. P. Pitaevskii, and S. Stringari, Phys. Rev. Lett. **106**, 185301 (2011).
[18] R. Liao and J. Brand, Phys. Rev. A **83**, 041604(R) (2011).
[19] A. Spuntarelli, L. D Carr, P. Pieri, and G. C Strinati, New J. Phys. **13**, 035010 (2011).
[20] R. G. Scott, F. Dalfovo, L. P. Pitaevskii, S. Stringari, O. Fialko, R. Liao, and J. Brand, New J. Phys. **14**, 023044 (2012).
[21] A. Cetoli, J. Brand, R. G. Scott, F. Dalfovo, and L. P. Pitaevskii, Phys. Rev. A **88**, 043639 (2013).
[22] P. Fulde and R. A. Ferrell, Phys. Rev. **135**, A550 (1964); A. I. Larkin and Yu. N. Ovchinnikov, Zh. Eksp. Teor. Fiz. **47**, 1136 (1964) [Sov. Phys. JETP **20**, 762 (1965)].
[23] N. Yoshida and S.-K. Yip, Phys. Rev. A **75**, 063601 (2007).
[24] X.-J. Liu, H. Hu, and P. D. Drummond, Phys. Rev. A **76**, 043605 (2007).
[25] M. M. Parish, S. K. Baur, E. J. Mueller, and D. A. Huse, Phys. Rev. Lett. **99**, 250403 (2007).
[26] R. M. Lutchyn, M. Dzero, and V. M. Yakovenko, Phys. Rev. A **84**, 033609 (2011).
[27] K. Sun and C. J. Bolech, Phys. Rev. A **85**, 051607(R) (2012).
[28] X.-W. Guan, M. T. Batchelor, and C. Lee, Rev. Mod. Phys. **85**, 1633 (2013).
[29] Y.-A. Liao, A. S. C. Rittner, T. Paprotta, W. Li, G. B. Partridge, R. G. Hulet, S. K. Baur, and E. J. Mueller, Nature (London) **467**, 567 (2010).
[30] C. Qu, M. Gong, and C. Zhang, Phys. Rev. A **89**, 053618 (2014).
[31] Y.-J. Lin, K. Jiménez-García, and I. B. Spielman, Nature (London) **471**, 83 (2011).
[32] P. Wang, Z.-Q. Yu, Z. Fu, J. Miao, L. Huang, S. Chai, H. Zhai, and J. Zhang, Phys. Rev. Lett. **109**, 095301 (2012).
[33] L. W. Cheuk, A. T. Sommer, Z. Hadzibabic, T. Yefsah,

W. S. Bakr, and M. W. Zwierlein, Phys. Rev. Lett. **109**, 095302 (2012).
[34] J.-Y. Zhang, S.-C. Ji, Z. Chen, L. Zhang, Z.-D. Du, B. Yan, G.-S. Pan, B. Zhao, Y.-J. Deng, H. Zhai, S. Chen, and J.-W. Pan, Phys. Rev. Lett. **109**, 115301 (2012).
[35] C. Qu, C. Hamner, M. Gong, C. Zhang, and P. Engels, Phys. Rev. A **88**, 021604(R) (2013).
[36] R. A. Williams, M. C. Beeler, L. J. LeBlanc, K. Jiménez-García, and I. B. Spielman, Phys. Rev. Lett. **111**, 095301 (2013).
[37] C. Zhang, S. Tewari, R. M. Lutchyn, and S. DasSarma, Phys. Rev. Lett. **101**, 160401 (2008).
[38] M. Sato, Y. Takahashi, and S. Fujimoto, Phys. Rev. Lett. **103**, 020401 (2009).
[39] S.-L. Zhu, L.-B. Shao, Z. D. Wang, and L.-M. Duan, Phys. Rev. Lett. **106**, 100404 (2011).
[40] L. Jiang, T. Kitagawa, J. Alicea, A. R. Akhmerov, D. Pekker, G. Refael, J. I. Cirac, E. Demler, M. D. Lukin, and P. Zoller, Phys. Rev. Lett. **106**, 220402 (2011).
[41] X.-J. Liu and H. Hu, Phys. Rev. A **85**, 033622 (2012).
[42] K. Seo, L. Han, and C. A. R. Sá de Melo, Phys. Rev. Lett. **109**, 105303 (2012).
[43] C. Nayak, S. H. Simon, A. Stern, M. Freedman, and S. DasSarma, Rev. Mod. Phys. **80**, 1083 (2008).
[44] N. Read and D. Green, Phys. Rev. B **61**, 10267 (2000); T. Mizushima, M. Ichioka, and K. Machida, Phys. Rev. Lett. **101**, 150409 (2008); L. Fu and C. L. Kane, Phys. Rev. Lett. **100**, 096407 (2008); R. M. Lutchyn, J. D. Sau, and S. DasSarma, Phys. Rev. Lett. **105**, 077001 (2010); Y. Oreg, G. Refael, and F. von Oppen, Phys. Rev. Lett. **105**, 177002 (2010); V. Mourik, K. Zuo, S. M. Frolov, S. R. Plissard, E. P. A. M. Bakkers, and L. P. Kouwenhoven, Science **336**, 1003 (2012); M. T. Deng, C. L. Yu, G. Y. Huang, M. Larsson, P. Caroff, and H. Q. Xu, Nano Lett. **12**, 6414 (2012); A. Das, Y. Ronen, Y. Most, Y. Oreg, M. Heiblum, and H. Shtrikman, Nat. Phys. **8**, 887 (2012); L. P. Rokhinson, X. Liu, and J. K. Furdyna, Nat. Phys. **8**, 795 (2012).
[45] A. Kitaev, Ann. Phys. (N. Y.) **303**, 2 (2003).
[46] J. Liu, A. C. Potter, K. T. Law, and P. A. Lee, Phys. Rev. Lett. **109**, 267002 (2012). The disorder can create the experimentally detected zero peak even for topological trivial systems.
[47] R. Sensarma, M. Randeria, and T.-L. Ho, Phys. Rev. Lett. **96**, 090403 (2006).
[48] Y. L. Loh and N. Trivedi, Phys. Rev. Lett. **104**, 165302 (2010).
[49] Y. Xu, C. Qu, M. Gong, and C. Zhang, Phys. Rev. A **89**, 013607 (2014).
[50] A. Y. Kitaev, Phys.-Usp. **44**, 131 (2001).
[51] G. Theocharis, D. J. Frantzeskakis, R. Carretero-González, P. G. Kevrekidis, B. A. Malomed, Phys. Rev. E **71**,017602 (2005).
[52] Y. Shin, C. H. Schunck, A. Schirotzek, and W. Ketterle, Phys. Rev. Lett. **99**, 090403 (2007).
[53] J. Liang, X. Zhou, P. Chui, K. Zhang, S.-J Gu, M. Gong, G. Chen, and S. Jia, arXiv:1404.3009.
[54] C. Qu, M. Gong, Y. Xu, S. Tewari, and C. Zhang, arXiv: 1310.7557.
[55] C. Hamner, J. J. Chang, P. Engels, and M. A. Hoefer, Phys. Rev. Lett. **106**, 065302 (2011).

SUPPLEMENTARY MATERIALS

In the main text, we show that there are four phases: NS, FFLO, PTS, and TS, instead of three in a homogeneous space. This extral PTS phase arises from the existence of a harmonic trap, where the chemical potential is replaced by a local one $\bar{\mu} = \mu - V(x)$ with the local density approximation. It is well known that a homogeneous spin-orbit coupled superfluid becomes topological when $V_z > \sqrt{\mu^2 + \Delta^2}$. In a harmonic trap, this relation can be approximately written as $V_z > \sqrt{\bar{\mu}^2 + \Delta(x)^2}$. Based on this relation, a superfluid can have a phase separation structure (i.e. PTS): a topological superfluid wing ($V_z > \sqrt{\bar{\mu}^2 + \Delta(x)^2}$ because of the smaller effective chemical potential $\bar{\mu}$) surrounding a normal superfluid core ($V_z < \sqrt{\mu^2 + \Delta(x)^2}$). This phase exists when $|\Delta| < V_z < \sqrt{\mu^2 + \Delta(0)^2}$. In Fig. S1, we present the order parameter profile $|\Delta(x)|$ and $\Delta V = V_z - \sqrt{\bar{\mu}^2 + \Delta^2}$ in a large region for three phases: (a) NS; (b) PTS; (c) TS. In the NS phase, V_z is so small that $V_z < \sqrt{\bar{\mu}^2 + \Delta(x)^2}$ in the whole space and there are no topological superfluids. As V_z is increased that $V_z > \sqrt{\bar{\mu}^2 + \Delta(x)^2}$ in the two shells as shown in Fig. S1 (b) so that superfluids become partially topological associated with two zero energy states. This transition can also be characterized by a sharp decrease of the minimum of the order parameter (i.e. Δ_1) at the topological superfluids region ($2x_s < x < 9x_s$) as illustrated in Fig. 2(b) in the main text. As V_z is furthur increased, $V_z > \sqrt{\mu^2 + \Delta(x)^2}$ and the whole superfluids become topological. In this phase, a soliton in the trap center hosts two Majorana fermions. Across the transition, the maximum of the order parameter (Δ_0) drops suddenly as shown in Fig. 2(b) in the main text.

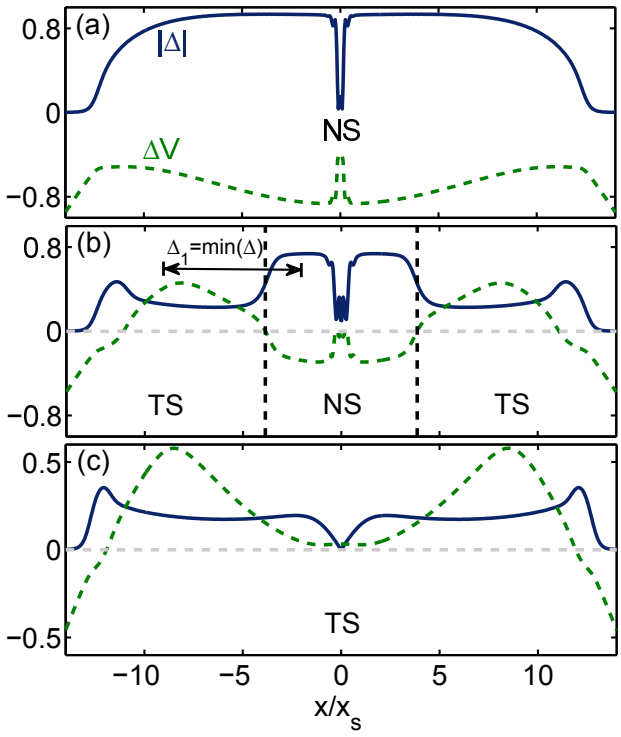

FIG. S1: (Color online) Plot of the order parameter profile $|\Delta(x)|$ and $\Delta V = V_z - \sqrt{\bar{\mu}^2 + \Delta(x)^2}$ in (a) for the NS phase with $V_z = 0.3E_F$, in (b) for the PTS phase with $V_z = 0.7E_F$, and in (c) for the TS phase with $V_z = 0.768E_F$. Here $\alpha K_F = E_F$ and $\Gamma = \pi$. Δ_1 is the minimum of the order parameter in region $2x_s < x < 9x_s$. The depletion at the center originates from the existence of a soliton.